

PAPER • OPEN ACCESS

New high-entropy oxide phases with the magnetoplumbite structure

To cite this article: V E Zhivulin *et al* 2021 *IOP Conf. Ser.: Mater. Sci. Eng.* **1014** 012062

View the [article online](#) for updates and enhancements.

You may also like

- [Carbon Modified \(CM\)- n-Fe₂O₃ Thin Films for Efficient Photoelectrochemical Splitting of Water](#)
Shahed U. Khan and Yasser A. Shaban
- [Tunable LiAlO₂/Al₂O₃ Coating to Improve the Specific Capacity and Cycle Stability of Nano-LiCoO₂](#)
Leon Shaw, Maziar Ashuri, Qianran He et al.
- [Atomic-Layer-Deposited Al₂O₃ as Gate Dielectrics for Graphene-Based Devices](#)
Bongki Lee, Greg Mordi, Taejoo Park et al.



ECS
The
Electrochemical
Society
Advancing solid state &
electrochemical science & technology

DISCOVER
how sustainability
intersects with
electrochemistry & solid
state science research

New high-entropy oxide phases with the magnetoplumbite structure

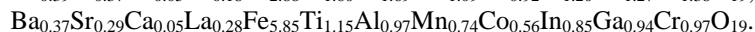
V E Zhivulin*, E A Trofimov, A Yu Starikov, S A Gudkova, A Yu Punda, D A Zherebtsov, O V Zaitseva and D A Vinnik

Department of Materials Science and Physical Chemistry of Materials, South Ural State University, Chelyabinsk, Russia

*Corresponding author: splav.zlat@mail.ru

Abstract. In the studied BaO–SrO–CaO–La₂O₃–Fe₂O₃–TiO₂–Al₂O₃–Mn₂O₃–CoO–In₂O₃–Ga₂O₃–Cr₂O₃ system there were synthesized three new high-entropy magnetoplumbite phases by solid-state sintering in air at 1300, 1350, and 1400 °C.

The average composition of the high-entropy phases obtained at 1350 °C can be described by the formulas:



The data obtained indicate that a significant portion of calcium was not incorporated into the high-entropy phase. This must be taken into account in the course of subsequent experimental work on the creation of homogeneous phases necessary for the study of their electrical and magnetic properties.

1. Introduction

In recent years, significant work has been carried out in obtaining novel non-metallic high-entropy systems [1-10]. The aim of our recent works is to study the possibility of obtaining multicomponent oxide phases with a magnetoplumbite structure, characterized by a high value of the configurational entropy of mixing [11-15]. Powder X-ray diffraction analysis of the samples allows us to confirm the phase purity of the created materials. Based on the obtained diffraction patterns, the parameters of the crystal lattice of the phases were calculated and a conclusion was made that these crystal structures belong to the magnetoplumbite structure (space group $P6_3/mmc$).

Such materials have potential applications in various areas of science and technology: in manufacturing permanent magnets, in magneto-optics, acoustoelectronics, microwave devices, and information storage devices. Studies carried out in recent decades have revealed that control of the properties of hexaferrites is possible by replacing some of the iron atoms with atoms of other elements [16-17]. Obtaining a high-entropy material with the magnetoplumbite structure opens up wide possibilities for smooth regulation of the entire complex of its electromagnetic characteristics, according to the demand of electronics manufacturers.

This work report the results of the synthesis of multicomponent phases with the magnetoplumbite structure in the BaO–SrO–CaO–La₂O₃–Fe₂O₃–TiO₂–Al₂O₃–Mn₂O₃–CoO–In₂O₃–Ga₂O₃–Cr₂O₃ system,



characterized by a high configuration entropy of mixing. It is assumed that a high entropy of mixing can stabilize multicomponent solid solutions with the magnetoplumbite structure.

2. Experiment

The synthesis was carried out in a system having the formula $(\text{Ba,Sr,Ca,La})\text{Fe}_x(\text{Ti,Al,Mn,Co,In,Ga,Cr})_{12-x}\text{O}_{19}$, where $x = 1.5, 3$ and 6 . It is obvious that the maximum configurational entropy in the sublattice formed by the elements Fe, Ti, Al, Mn, Co, In, Ga, and Cr is achieved when the concentrations of all these elements are equal to $x = 1.5$. However, in this work, we also investigated compositions having a larger iron fraction than the fraction of the other elements of B type (in a general formula $\text{AB}_{12}\text{O}_{19}$). An increase of the iron content will lead to a slight decrease in the configurational entropy of mixing (ΔS_{conf}); however, compositions with larger iron content are of higher interest from the point of view of potential applications of the materials obtained. The batch compositions for solid-state sintering were calculated in accordance with the above formula (table 1).

Table 1. Batch compositions of $(\text{Ba,Sr,Ca,La})\text{Fe}_x(\text{Ti,Al,Mn,Co,In,Ga,Cr})_{12-x}\text{O}_{19}$ samples.

	Sample number		
	1	2	3
x Fe	1.5	3	6
BaCO ₃ , wt. %	4.247	4.274	4.329
SrCO ₃ , wt. %	3.177	3.197	3.239
CaCO ₃ , wt. %	2.154	2.168	2.196
La ₂ O ₃ , wt. %	3.506	3.528	3.574
Fe ₂ O ₃ , wt. %	10.310	20.752	42.040
TiO ₂ , wt. %	10.313	8.896	6.007
Al ₂ O ₃ , wt. %	6.583	5.679	3.835
Mn ₂ O ₃ , wt. %	10.193	8.792	5.937
CoO, wt. %	9.676	8.346	5.636
In ₂ O ₃ , wt. %	17.925	15.463	10.442
Ga ₂ O ₃ , wt. %	12.102	10.439	7.049
Cr ₂ O ₃ , wt. %	9.813	8.465	5.716

The following reagents were used for the experiments: BaCO₃, SrCO₃, CaCO₃, La₂O₃, Fe₂O₃, TiO₂, Mn₂O₃, CoO, In₂O₃, Cr₂O₃, Ga₂O₃, Al₂O₃ of analytical grade purity.

Weighed portions of reagents were thoroughly mixed, pressed into tablets, and heated in air in a SiC furnace at 1300, 1350, or 1400 °C for 5 hours. After heat treatment, the sintered samples were crashed, and the fracture surfaces were examined using a Jeol JSM7001F scanning electron microscope equipped with an Oxford INCA X-max 80 X-ray spectrometer for elemental analysis. In order to confirm the structure, the obtained samples were investigated by X-ray phase analysis using a Rigaku Ultima IV X-ray powder diffractometer.

3. Results and discussions

Typical microcrystals found in the samples are presented in figure 1. The averaged results of X-ray spectral analysis of hexagonal microcrystals are listed in table 2. The compositions are presented as the average number of metal atoms per 13 metal atoms in the formula unit. In addition to the elemental

analysis data, the table shows the target compositions (when the batch components would be completely incorporated into the magnetoplumbite phase).

From the data presented, it can be seen that the ratio between the number of atoms of type B and the number of atoms of type A in hexagonal crystals of all samples is quite close to 12. This ratio, as well as the data of X-ray phase analysis, indicate that solid-state synthesis enables obtaining high-entropy phases with the magnetoplumbite structure.

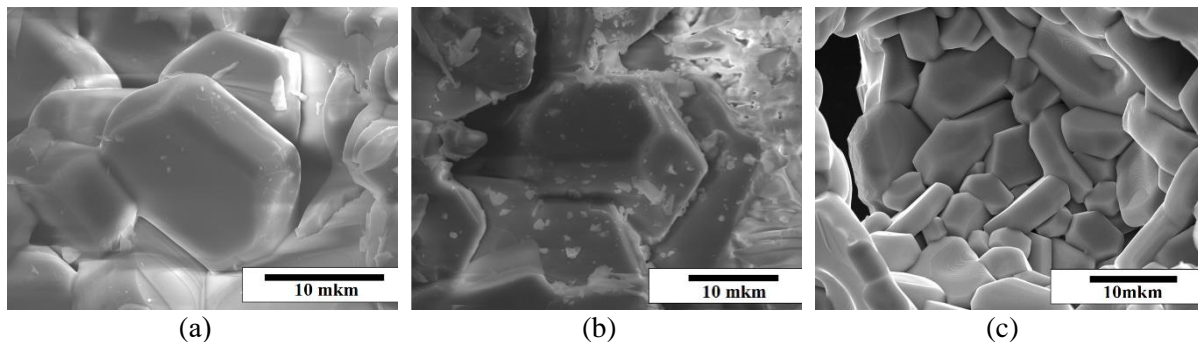
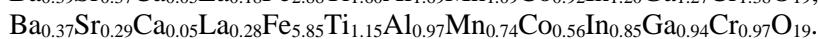
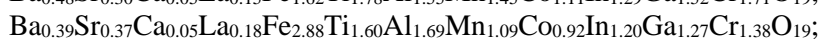


Figure 1. Morphology of crystals found in the samples: (a) composition 1, 1350 °C; (b) composition 2, 1400 °C; (c) composition 3, 1300 °C.

High-entropy magnetoplumbite phases were formed at all three temperatures used for synthesis. The obtained micrographs (figure 1) show that at higher temperatures, the average size of the formed hexagonal crystals increases. At the same time, an increase in temperature leads to the appearance of a larger number of molten areas, as well as particles of irregular shape.

The average composition of high-entropy phases in samples obtained at 1350 °C can be described by the formulas:



The data obtained indicate that under the experimental conditions a large amount of calcium was not incorporated into the high-entropy phase. This fact must be taken into account considering subsequent syntheses of homogeneous phases necessary for the study of their electrical and magnetic characteristics. Probably, the optimal composition of the batch for the synthesis should be chosen from the compositions of the formed phases (table 2).

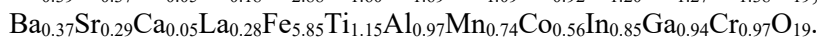
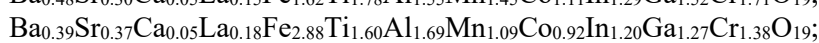
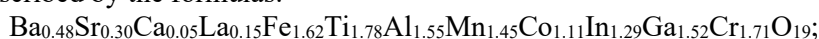
Table 2. Averaged results of hexagonal crystals elemental analysis (the atomic fractions are presented as its number normalized by 13 atoms).

Sample number	[A] (for $\text{AB}_{12}\text{O}_{19}$)				[B] (except [Fe] for $\text{AB}_{12}\text{O}_{19}$)							
	[Ba]	[Sr]	[Ca]	[La]	[Al]	[Ti]	[Cr]	[Mn]	[Co]	[Ga]	[In]	[Fe]
1 (batch)	0.25	0.25	0.25	0.25	1.5	1.5	1.5	1.5	1.5	1.5	1.5	1.5
1(experiment)	0.47	0.30	0.05	0.15	1.54	1.78	1.71		1.11	1.51	1.28	1.61
	6	0	1	2	5	4	3	1.445	0	8	7	9
2 (batch)	0.25	0.25	0.25	0.25	1.28	1.28	1.28	1.286	1.28	1.28	1.28	3
					6	6	6		6	6	6	
2(experiment)	0.38	0.36	0.05	0.17	1.68	1.59	1.37		0.92	1.26	1.19	2.87
	9	7	0	6	8	7	5	1.093	2	7	9	9

3 (batch)	0.25	0.25	0.25	0.25	0.85	0.85	0.85	0.857	0.85	0.85	0.85	6
					7	7	7		7	7	7	
3(experiment)	0.37	0.29	0.05	0.27	0.96	1.14	0.96		0.56	0.93	0.84	5.84
	1	1	3	8	9	6	5	0.736	1	6	7	8

4. Conclusions

During the study of the BaO–SrO–CaO–La₂O₃–Fe₂O₃–TiO₂–Al₂O₃–Mn₂O₃–CoO–In₂O₃–Ga₂O₃–Cr₂O₃ system, the new high-entropy phases with the magnetoplumbite structure were obtained by solid-state sintering. The average composition of these phases obtained at a temperature of 1350 °C can be described by the formulas:



Conclusions are drawn about the possible directions for obtaining homogeneous samples.

Acknowledgments

The work was supported by the Russian Science Foundation (project No. 18-73-10049).

References

- [1] Rost C, Sachet E, Borman T, Moballegh A, Dickey E, Hou D, Jones J, Curtarolo S and Maria JP 2015 *Nat. Commun.* **6** 8485
- [2] Bérardan D, Franger S, Dragoë D, Meena A and Dragoë N *Phys. Status Solidi RRL* 2016 **10** pp 328–33
- [3] Sarkar A, Djenadic R, Usharani N, Sanghvi K, Chakravadhanula V, Gandhi A, Hahn H and Bhattacharya S 2017 *J. Eur. Ceram. Soc.* **37** pp 747–54
- [4] Berardan D, Franger S, Meena A and Dragoë N 2016 *J. Mater. Chem. A* **4** pp 9536–41.
- [5] Rak Z, Rost C, Lim M, Sarker P, Toher C, Curtarolo S, Maria J P and Brenner D 2016 *J. Appl. Phys.* **120** 9
- [6] Rost C, Rak Z, Brenner D and Maria J P 2017 *J. Am. Ceram. Soc.* **100** pp 2732–38
- [7] Berardan D, Meena A K, Franger S, Herrero C and Dragoë N 2017 *J. Alloys Compd.* **704** pp 693–700
- [8] Sarkar A, Loho C, Velasco L, Thomas T, Bhattacharya S S, Hahn H and Djenadic R 2017 *Dalton Trans.* **46** pp 12167–76
- [9] Djenadic R, Sarkar A, Clemens O, Loho C, Botros M, Chakravadhanula V S, Kübel C, Bhattacharya S, Gandhi A and Hahn H 2017 *Mater. Res. Lett.* **5** pp 102–09
- [10] Lin M I, Tsai M H, Shen W J and Yeh J W 2019 *Thin Solid Films* **518** pp 2732–37
- [11] Zaitseva O, Vinnik D and Trofimov E, 2019 *Mater. Sci. Forum* **946** pp 186–91
- [12] Vinnik D, Zhivulin V, Trofimov E, Starikov A, Zherebtsov D, Zaitseva O, Gudkova S, Taskaev S, Klygach D, Vakhitov M, Sander E, Sherstyuk D and Trukhanov A 2019 *Nanomaterials* **9** 559
- [13] Vinnik D, Trofimov E, Zhivulin V, Zaitseva O, Gudkova S, Starikov A, Zherebtsov D, Kirsanova A, Häbner M and Niewa R 2019 *Ceram. Int.* **45** pp 12942–48
- [14] Vinnik D, Trofimov E, Zhivulin V, Zaitseva O, Zherebtsov D, Starikov A, Sherstyuk D, Gudkova S and Taskaev S 2020 *Ceram. Int.* **46** pp 9656–9660
- [15] Vinnik D, Trukhanov A, Podgornov F, Trofimov E, Zhivulin V, Starikov A, Zaitseva O, Gudkova S, Kirsanova A, Taskaev S, Uchaev D, Trukhanov S, Almessiere M, Slimani Y. and Baykal A 2020 *J. Eur. Ceram. Soc.* **40** pp 4022–28
- [16] Vinnik D, Ustinova I, Ustinov A, Gudkova S, Zherebtsov D, Trofimov E, Zabeivorota N, Mikhailov G and Niewa R 2017 *Ceram. Int.* **17** pp 15800–04
- [17] Pullar R C 2012 Hexagonal ferrites: A review of the synthesis, properties and applications of hexaferrite ceramics *Prog. Mater. Sci.* **57** pp 1191–1334